

Article

Imaging Spectroscopic Analysis of Biochemical Traits for Shrub Species in Great Basin, USA

Yi Qi ^{1,*} , Susan L. Ustin ²  and Nancy F. Glenn ³ ¹ School of Natural Resources, University of Nebraska-Lincoln, Lincoln, NE 68583, USA² Center for Spatial Technologies and Remote Sensing (CSTARS), Department of Land, Air and Water Resources, University of California, Davis, CA 95616, USA; slustin@ucdavis.edu³ Department of Geosciences, Boise State University, Boise Center Aerospace Lab, 1910 University Drive, Boise, ID 83725, USA; nancyglenn@boisestate.edu

* Correspondence: yi.qi@unl.edu; Tel.: +1-402-472-8195

Received: 4 September 2018; Accepted: 10 October 2018; Published: 12 October 2018



Abstract: The biochemical traits of plant canopies are important predictors of photosynthetic capacity and nutrient cycling. However, remote sensing of biochemical traits in shrub species in dryland ecosystems has been limited mainly due to the sparse vegetation cover, manifold shrub structures, and complex light interaction between the land surface and canopy. In order to examine the performance of airborne imaging spectroscopy for retrieving biochemical traits in shrub species, we collected Airborne Visible Infrared Imaging Spectrometer—Next Generation (AVIRIS-NG) images and surveyed four foliar biochemical traits (leaf mass per area, water content, nitrogen content and carbon) of sagebrush (*Artemisia tridentata*) and bitterbrush (*Purshia tridentata*) in the Great Basin semi-desert ecoregion, USA, in October 2014 and May 2015. We examined the correlations between biochemical traits and developed partial least square regression (PLSR) models to compare spectral correlations with biochemical traits at canopy and plot levels. PLSR models for sagebrush showed comparable performance between calibration (R^2 : LMA = 0.66, water = 0.7, nitrogen = 0.42, carbon = 0.6) and validation (R^2 : LMA = 0.52, water = 0.41, nitrogen = 0.23, carbon = 0.57), while prediction for bitterbrush remained a challenge. Our results demonstrate the potential for airborne imaging spectroscopy to measure shrub biochemical traits over large shrubland regions. We also highlight challenges when estimating biochemical traits with airborne imaging spectroscopy data.

Keywords: imaging spectroscopy; biochemical traits; dryland ecosystem; shrub species; AVIRIS-NG

1. Introduction

The biochemical traits of plant foliage provide important information to study photosynthetic capacity and biogeochemical cycling in ecosystems [1–5]. Among widely-studied biochemical traits are leaf mass per area, water content, nitrogen content, and carbon content. Variations in leaf mass per area (LMA, ratio of leaf dry mass to leaf area) correspond to the fundamental tradeoffs in leaf construction costs vs. light-intercepting surface area and are driven by a range of environmental controls [6,7]. While foliage gains carbon and builds structure, LMA corresponds to several biochemical and structural compounds in the plant including (positive correlation) cellulose and lignin, and (negative correlation) protein. These relate to physiological processes of photosynthesis, primary production and leaf decomposition [8,9]. Water is one of the most important factors regulating plant growth and development in ecosystems [10]. Leaf water content is an important parameter for assessing drought and predicting susceptibility of wildfire. Nitrogen content is a fundamental component of

light-harvesting pigments and photosynthetic machinery, and it is closely related to the maximum photosynthetic rate [11,12].

Remote sensing provides an opportunity to assess plant biochemical traits across large areas compared to field sampling methods. Multispectral satellite sensors like MODIS and Landsat have been used to monitor vegetation properties, and airborne imaging spectrometers have proven useful for mapping variation in the spatial distribution of plant biochemical traits mainly attributed to narrow spectral bands, fine spatial resolution and continuous reflectance measurement in solar spectra [13,14]. Relationships between canopy biochemical traits and airborne imaging spectroscopy have been demonstrated in a variety of ecosystems, such as tropical forests [15,16], northern temperate and boreal tree species [17,18], Mediterranean species in California [19,20], and northwest [21] and northeast forests [22] in the U.S. Although previous studies have demonstrated the potential for measuring plant biochemical traits from reflectance spectra, there are still shortages and challenges in the remote sensing of biochemical traits in dryland ecosystems.

First, spectral determination of biochemical traits of shrub species in dryland ecosystems has been difficult mainly due to the complex variation in vegetation structure from pixel to landscape levels [23]. Dryland ecosystems usually have low-stature; sparse vegetation cover; an abundance of targets with high albedo [24,25]; and complex spectral mixing functions between visible, near-infrared and shortwave infrared wavelengths [26]. Although various statistical methods have been used to estimate traits with reflectance spectra [15,27–29], there is a need for a more comprehensive examination of spectral correlation with traits in regression models.

Second, although there are previous studies examining imaging spectroscopy instruments for measuring certain traits in shrub species, limited studies have investigated the performance of new imaging spectroscopy instruments to assess a series of vegetation traits. Airborne Visible Infrared Imaging Spectrometer (AVIRIS) data in the USA have shown the potential to derive water content [30, 31] and nitrogen content [19]. Mirik et al. [32] investigated 1-m resolution PROBE-1 hyperspectral imagery system (Earth Search Sciences Inc. Kalispell, MT, USA) to estimate nitrogen, phosphorus and neutral detergent fiber in a range of shrub species in Yellowstone National Park. Mitchell et al. [33] examined HyMap sensor data (HyVista, Inc., Sydney, Australia) to estimate foliar and canopy nitrogen content in sagebrush. Airborne Visible Infrared Imaging Spectrometer Next Generation (AVIRIS-NG) has been developed to replace the AVIRIS instrument that has been flying since 1986. Similarly, the National Ecological Observatory Network (NEON, <http://www.neonscience.org/>, last accessed in August 2018) integrates an AVIRIS-NG sensor and field sites to measure numerous vegetation metrics across eco-climatic domains in the U.S. The increased availability and sensor characteristics of platforms such as AVIRIS-NG have the potential to more broadly examine shrub biochemical traits and monitor long-term changes in dryland ecosystems.

Third, dryland ecosystems account for roughly 41% of the Earth's surface and support 38% of the world's current population [34]. The Great Basin, a semi-arid ecoregion, is representative of the dryland ecosystem in the western U.S. It has experienced multiyear drought accompanied with concerns that include long term aridity, biodiversity loss, and increased regional fire activity [35,36]. The 2012–2015 drought has left severe canopy water loss in California and substantial future forest change [37]. Xue et al. [38] indicated that annual total precipitation and extreme precipitation days showed a significant positive trend in the eastern Great Basin during 1951–2013, while the western basin experienced significant negative trends. The western Great Basin might experience a drier and sparser shrub community if the trend continues. Great Basin sagebrush (*Artemisia tridentata*) and bitterbrush (*Purshia tridentata*), two widely distributed species in Great Basin ecoregion, play critical roles in the hydrologic cycle and in sustaining wildlife and livestock. Examining biochemical traits in these species will provide insights to study plant productivity and biogeochemical cycling in the Great Basin.

The primary objective of this research is to investigate imaging spectroscopy approaches for estimating key biochemical traits in shrub species in the Great Basin. We aim to examine three specific

aspects: (i) The variation and correlation of biochemical traits within and between shrub species, (ii) the performance of airborne imaging spectrometer AVIRIS-NG for measuring biochemical traits, and (iii) the modeling complexity at canopy and plot levels. To answer these questions we collected shrub samples for biochemical traits in representative sagebrush and bitterbrush communities concurrent with AVIRIS-NG flights. Then we examined the correlation between traits and developed partial least square regression (PLSR) models to evaluate spectral correlation at canopy and plot levels.

2. Materials and Data

2.1. Study Sites

We selected two sites on the eastern slopes of the Sierra Nevada Mountains, in Owens Valley, CA, USA (Figure 1a). One site was located on large depositional fans (bajadas) out of the Sierra Nevada Mountains and represents the southern extent of sagebrush communities in the region. The other site was farther south and is near the southern end of a long ecotone that transitions into the Mojave Desert ecosystem. The two sites span a geographic region approximately 57 km² at elevations between 1215 m and 1892 m. The study areas are within the rain shadow of the Sierra Nevada Mountains and consist of a diverse mixture of semiarid vegetation communities. The continental climate has cold winters with hot summers, with a precipitation regime dominated by winter storms. The total annual precipitation was about 9.6 cm in 2014 and 6.9 cm in 2015.

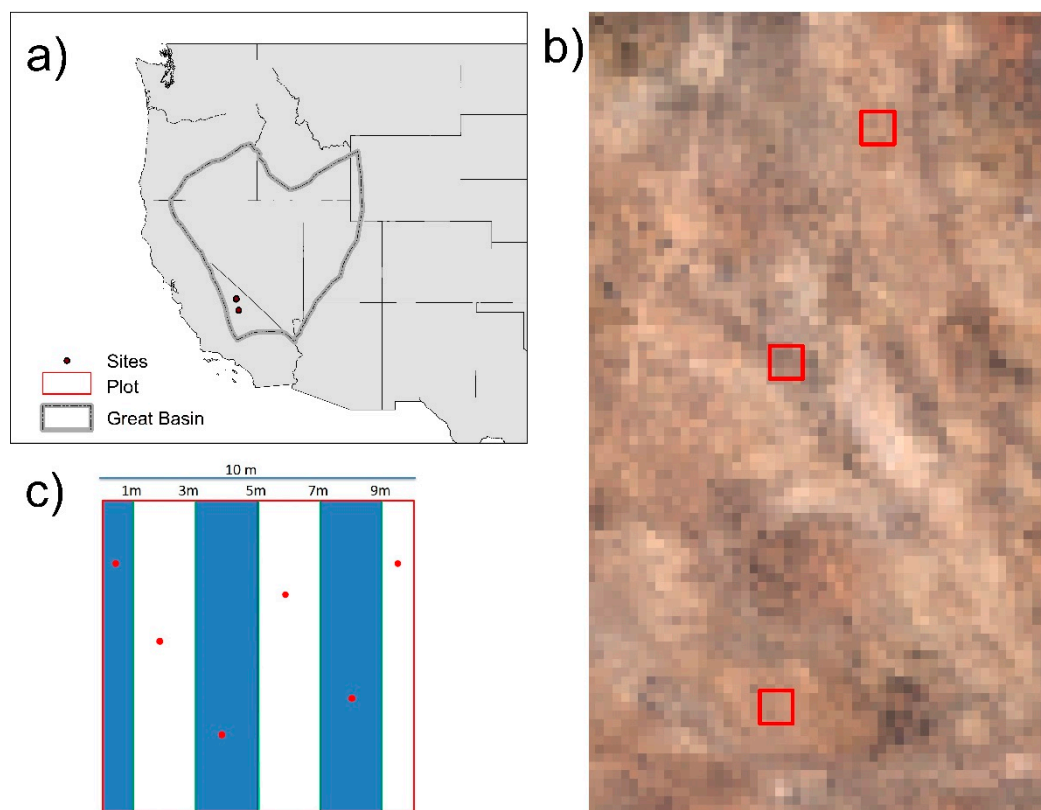


Figure 1. (a) Location of two research sites in California, USA; (b) examples of plots (red boxes) overlaid on top of AVIRIS-NG true color images; (c) field sampling scheme in 10 × 10 m plots. Blue strips represent spaces between line transects, and red dots represent sampled shrubs between intersects.

The vegetation community in our study area is complex due to heterogeneous soil types, rocks, and disturbances including grazing, wildfires, and the regional drought in years 2012–2016. Most of the Sierra Nevada fan vegetation is a mix of Great Basin sagebrush (*Artemisia tridentata*) semi-desert ecosystem type and bitterbrush (*Purshia tridentata*) and Blackbrush (*Coleogyne ramosissima*) transitional

type, while the valley floor is dominated by alkali grasslands (*Distichlis spicata*, *Sporobolus airoides*) and saltbush (*Atriplex* sp., *Sarcobatus vermiculatus*) communities.

2.2. Field Data Collection

We established 10 × 10 m plots (north-south orientation) in October 2014 and revisited them in May 2015 (Figure 1b). These plots represented relatively homogenous patches of sagebrush and bitterbrush. Within each plot we set up 10-m-long line transects at 1, 3, 5, 7, 9 m intervals (Figure 1c), then we recorded shrub species; shrub canopy coverage length along each transect; calculated the percentage of shrub cover on each transect by dividing the coverage length by 10 m; and then averaged shrub covers of five transects as the plot shrub cover (%). We randomly chose one shrub between each transect if a shrub was present. We recorded the GPS locations of chosen shrubs and the four corners of each plot with a Trimble GeoExplorer® 7 series GPS. For every chosen shrub we measured the major (widest) canopy width, minor (narrowest) canopy width (in meter), and leaf area index (LAI) with a LI-COR plant canopy analyzer (LAI-2200 model); then we randomly collected four branch tips (3–5 cm) from the canopy. All samples were immediately stored in sealed plastic bags in a cooler with ice and transported to the laboratory to carry out biochemical analysis. In total, we sampled 17 sagebrush plots (99 shrubs) and 12 bitterbrush plots (50 shrubs) in 2014, 18 sagebrush plots (95 shrubs) and 12 bitterbrush plots (24 shrubs) due to shrub mortality in 2015.

2.3. Biochemical Measurements

Within 12 h after sample collection we removed the leaves from the sampled branch tips and weighed the fresh leaf mass. Four branch tips from each shrub were mixed to represent one sample for that shrub. Then we laid the leaves on a flat-bed scanner and recorded grayscale scanned images. The leaf area (cm²) was calculated as the ratio of the number of black pixels to the total number of pixels. The leaves were dried in a convection oven for 24 h at 60 degree centigrade and re-weighed to determine dry mass. Water mass was calculated as the difference between fresh leaf mass and dry mass. Foliar LMA (mg/cm²) was determined by dividing dry leaf mass by leaf area, and water content (mg/cm²) was calculated as the ratio of water mass to leaf area. Then the dried leaves were ground to measure nitrogen and carbon percentage (% of dry mass) using combustion-gas chromatography (Costech ECS 4010).

2.4. Remote Sensing Data

On 9 October 2014, and 13 June 2015, the AVIRIS-NG collected images of our study area with a nominal pixel resolution of 2.6 m. The AVIRIS-NG instrument measures the spectral radiance at the wavelength range from 380 nm and 2510 nm with 5 nm sampling [39]. The raw images were orthorectified, calibrated to radiance, and atmospherically corrected to surface reflectance based on Atmosphere Removal Algorithm (ATREM) program [40]. The individual shrub canopy-level spectra were extracted from pixels at the GPS locations on the imagery after removal of the following wavebands due to noise and water vapor absorptions: 346–391 nm, 1348–1428 nm, 1778–1949 nm, 2485–2510 nm. The plot-level spectra were averaged spectra of pixels within each 10 × 10 m plot area.

2.5. Data Analysis

We pooled foliar biochemical traits and shrub spectra from 2 years. Then we calculated correlation coefficients between pairs of biochemical traits in each species to analyze correlations between traits. Partial least squares regression (PLSR) is a widely used multivariate statistical method in chemometrics and near-infrared spectroscopy for analyzing quantitative relationships between multiple predictor and response variables [41]. PLSR has been a valuable method in spectroscopy for analyzing quantitative relationships between reflectance data and vegetation biochemical traits [15,17,33,42]. We implemented a bootstrap method to develop a single response PLSR model between each biochemical trait and spectra by species. In each species dataset, we first used the Kennard-Stone algorithm to divide the

dataset into 80% training and 20% for validation [43]. The Kennard-Stone algorithm uses a uniform mapping method to ensure both training and validation datasets provide uniform coverage of the entire dataset [43]. We further implemented 500 iterations by randomly selecting 80% of the calibration dataset to build a PLSR model with leave-one-out validation. The optimal number of PLSR components was determined when the prediction residual sum of squares (PRESS) was minimized, and successive PLSR components did not improve the root mean square error in prediction (RMSEP) as assessed using a *t*-test [44]. Lastly, we applied 500 PLSR models from the calibration dataset with the determined number of components on the validation dataset. To enable comparison between models, we calculated the mean and standard deviation of *R*-square (R^2) and relative root mean square error (divide RMSE by the range of observation values) to measure modeling accuracy in the calibration and validation models. We also calculated the mean of variable importance in the projection (VIP) metric to identify regions of the reflectance spectra that were significant in the 500 calibration models. VIP is a weighted sum of squares of the PLSR weights with the weights calculated from the amount of variance in response variables of each PLSR component. Higher absolute VIP values indicate great importance for wavelengths in projecting traits. Generally, the wavelengths with VIP values larger than 1 are considered important [45]. In plot-level models, we calculated biochemical traits as the mean leaf traits of sampled shrubs within each plot, and then we implemented the same PLSR analytic workflow as the canopy-level models.

3. Results

3.1. Variation in Biochemical Traits and Reflectance

The biochemical traits showed variation between years and species (Table 1). In general, foliar traits showed higher LMA and carbon content, and lower water and nitrogen content in October 2014 than in May 2015. LMA and water in sagebrush presented smaller means than bitterbrush. Two species had similar canopy measurements including LAI, major and minor widths. Correlation analyses showed correlation coefficients between pairs of canopy biochemical traits (Table 2). While most correlations were not significant, LMA and water content showed positive correlation in the sagebrush, and LMA and carbon content showed positive correlation in the bitterbrush.

Table 1. Mean and standard deviation (in parenthesis) of foliar biochemical traits, leaf area index, major width, minor width, and vegetation cover of sagebrush and bitterbrush.

	Sagebrush		Bitterbrush	
	2014	2015	2014	2015
LMA (mg/cm ²)	13.36 (3.24)	8.67 (1.82)	21.52 (3.92)	18.22 (2.26)
Water (mg/cm ²)	9.24 (3.59)	9.79 (2.49)	14.73 (2.91)	14.82 (2.38)
Nitrogen (%)	2.09 (0.27)	2.43 (0.28)	1.49 (0.13)	1.56 (0.16)
Carbon (%)	51.56 (1.51)	49 (1.27)	50.27 (1.43)	50.24 (1.12)
LAI	1.91 (0.46)	1.98 (0.49)	1.99 (0.43)	1.91 (0.59)
Major Width (m)	1.68 (0.71)	1.25 (0.46)	1.47 (0.94)	1.40 (0.57)
Minor Width (m)	1.24 (0.54)	1.13 (1.49)	1.39 (1.33)	1.17 (0.51)
Vegetation Cover	0.34 (0.13)	0.33 (0.17)	0.14 (0.12)	0.13 (0.1)

Table 2. Correlation coefficients between pairs of canopy biochemical traits.

	Water	LMA	Nitrogen	Carbon
Water	1.00 (1.00)			
LMA	0.60 * (−0.01)	1.00 (1.00)		
Nitrogen	0.19 (−0.01)	−0.13 (0.08)	1.00 (1.00)	
Carbon	−0.20 (−0.15)	−0.05 (0.31 *)	−0.03 (−0.14)	1.00 (1.00)

Note: Coefficients outside parenthesis are from sagebrush, and inside are from bitterbrush. Asterisks denote significant level of 0.05.

The reflectance spectra varied in association with the biochemical traits at both shrub canopy and plot levels (Figure 2). The extracted spectra were from pixels mixed with features like background soil and dry grass. In contrast with typical mesic green leaf spectra, shrubs did not show a strong pattern of pigment absorption in the visible wavelengths. High reflectance in the near infrared and shortwave infrared wavelengths indicated the water-stressed vegetation, abundant dry biomass in stems and litter and bright soils in the background.

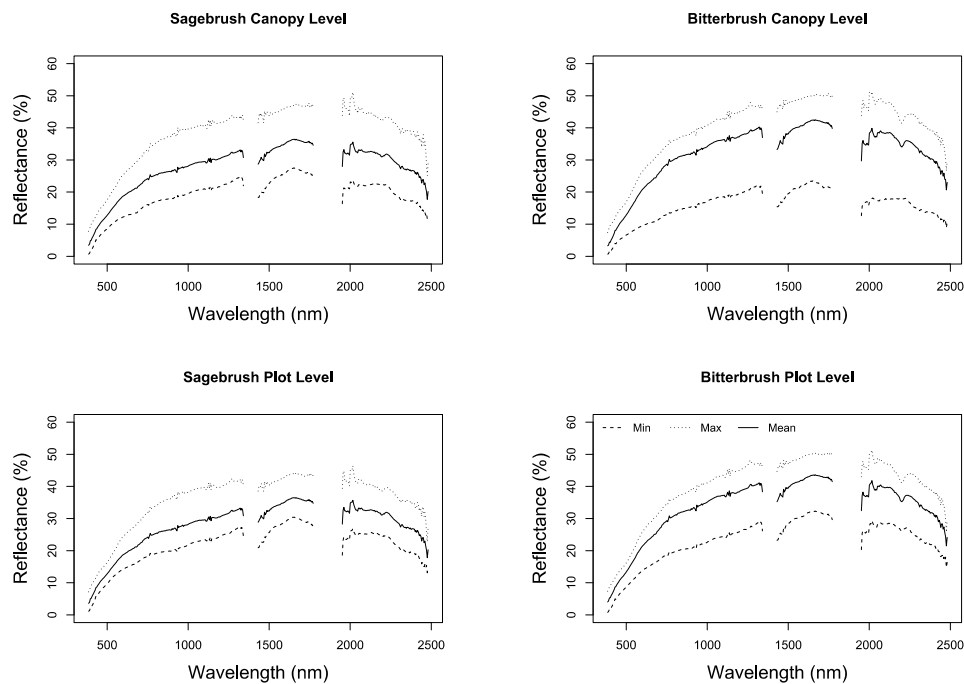


Figure 2. The mean, minimum and maximum reflectance spectra of sagebrush and bitterbrush at canopy level and 10×10 m plots of two species.

3.2. PLSR Analysis

PLSR models of sagebrush produced comparable accuracy between calibration and validation in all biochemical traits at the canopy level (Table 3). The R^2 values in the calibration models were above 0.4 for all traits. Validation models generally showed smaller R^2 and larger rRMSE in comparable ranges as calibration models (Figure 3). For bitterbrush, calibration models in LMA and nitrogen could not predict the validation dataset, and R^2 in the water validation model was small. PLSR models also identified high VIP values (larger than 1) at spectral regions associated with biochemical traits (Figure 4).

Table 3. Results of PLSR canopy-level biochemical traits in sagebrush and bitterbrush.

		Calibration		Validation	
		R^2 (S.D.)	rRMSE (S.D.)	R^2 (S.D.)	rRMSE (S.D.)
Sagebrush ($n = 194$)	LMA	0.66 (0.04)	3.28 (0.39)	0.52 (0.01)	2.69 (0.01)
	Water	0.70 (0.03)	3.98 (0.37)	0.41 (0.06)	8.24 (0.08)
	Nitrogen	0.42 (0.04)	1.57 (0.02)	0.23 (0.05)	1.76 (0.01)
	Carbon	0.60 (0.03)	1.10 (0.01)	0.57 (0.02)	1.09 (0.01)
Bitterbrush ($n = 74$)	LMA	0.86 (0.04)	1.72 (0.11)	-	-
	Water	0.51 (0.06)	2.04 (0.18)	0.06 (0.17)	2.34 (0.03)
	Nitrogen	0.04 (0.04)	1.49 (0.05)	-	-
	Carbon	0.17 (0.06)	1.09 (0.01)	0.27 (0.06)	1.07 (0.01)

Note: R -square (R^2), relative root mean square error (rRMSE), and standard deviation (S.D.) are from the calibration and validation models respectively. Dash lines denote results that are not significant.

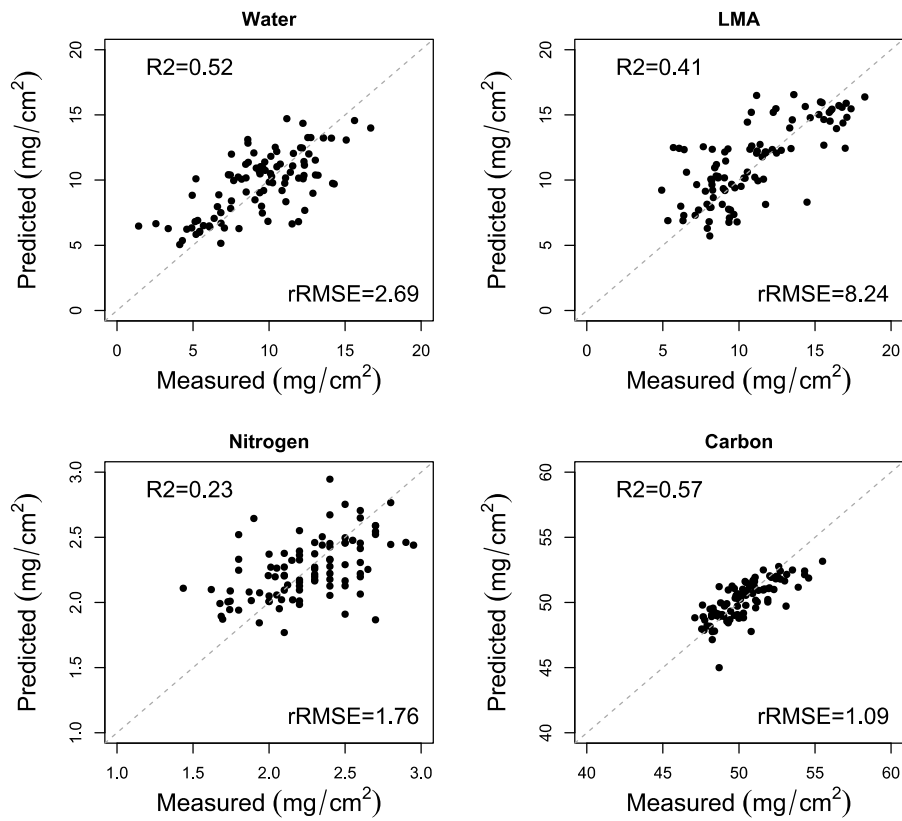


Figure 3. Comparisons between the measured and predicted traits in canopy PLSR validation model of sagebrush. The dashed line is 1:1 line.

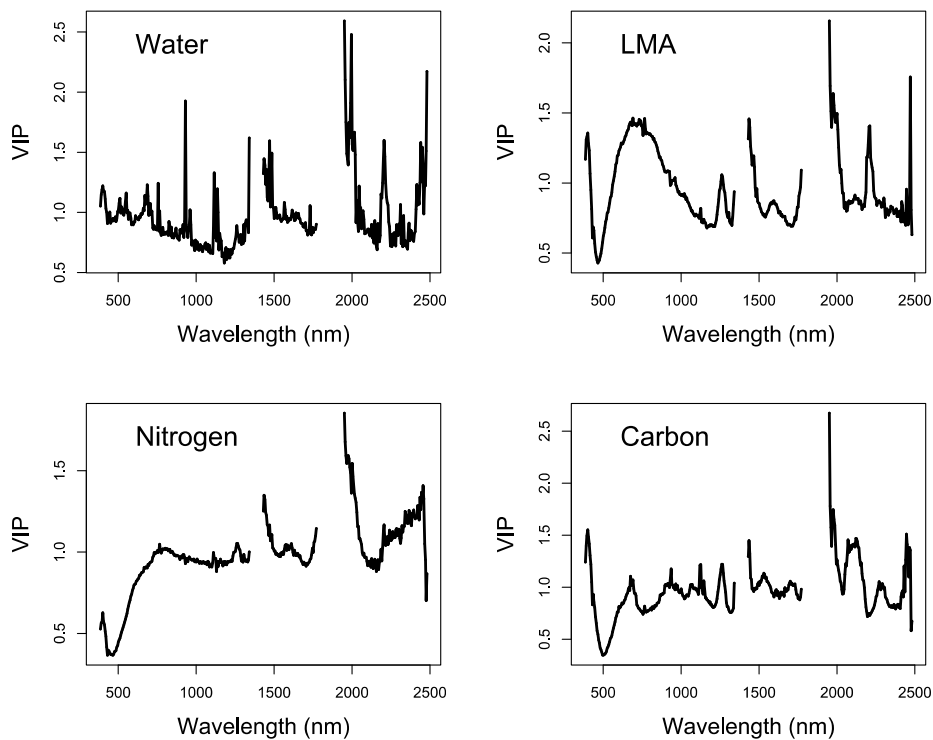


Figure 4. Mean variable importance in projection (VIP) values of the canopy-level PLSR calibration models in sagebrush.

The plot-level PLSR models showed that the reflectance spectra could model biochemical traits (Table 4). PLSR calibration data generally produced higher or comparable R^2 and smaller rRMSE values than validation data in sagebrush plots. The rRMSE of nitrogen and water models were larger than values of LMA and water models. In bitterbrush plots, only water content could be modeled in comparable accuracy between calibration and validation data.

Table 4. Results of PLSR plot-level biochemical traits in sagebrush and bitterbrush.

		Calibration		Validation	
		R^2 (S.D.)	rRMSE (S.D.)	R^2 (S.D.)	rRMSE (S.D.)
Sagebrush ($n = 35$)	LMA	0.73 (0.09)	1.31 (0.11)	0.67 (0.06)	1.32 (0.01)
	Water	0.67 (0.07)	1.19 (0.11)	0.1 (0.11)	1.49 (0.02)
	Nitrogen	0.66 (0.08)	3.04 (0.24)	0.52 (0.04)	2.75 (0.01)
	Carbon	0.7 (0.06)	9.26 (1.16)	0.38 (0.04)	9.17 (0.01)
Bitterbrush ($n = 24$)	LMA	0.81 (0.05)	2.07 (0.18)	0.08 (0.05)	1.94 (0.02)
	Water	0.81 (0.08)	2.47 (0.58)	0.68 (0.13)	2.74 (0.01)
	Nitrogen	0.12 (0.11)	2.94 (0.83)	–	–
	Carbon	0.8 (0.1)	13.97 (2.26)	–	–

Note: R -square (R^2), relative root mean square error (rRMSE), and standard deviation (S.D.) are from the calibration and validation models respectively. Dash lines denote results that are not significant.

4. Discussion

Our study sites represent a typical sagebrush and bitterbrush dominant community in the Great Basin, albeit sites are at the extreme southwest boundary of this vegetation type, into the ecotone transition with the warmer and drier Mojave Desert ecosystem. Our sampling dates were long after the rainy season ended in both 2014 and 2015, and the severe drought in California had significantly stressed forests and rangelands throughout southern Sierra Nevada, to produce extensive mortality [37]. Leaf water content changes seasonally between 75% and 45% of fresh weight in shrub species [42], but water in our samples averaged about 46% by fresh weight in sagebrush and 42% in bitterbrush. These low values of leaf water content are consistent with the drought conditions during both years of this project, indicating a high degree of water stress on the plants [46]. The variation in foliar traits across years represented a seasonal variation in the plant physiological process and environment. As shrubs grew from spring to fall, foliar LMA and carbon content increased, but water and nitrogen content decreased. Shrubs utilized nitrogen to construct the foliar structure, likely resulting in higher LMA, and water resource scarcity during the summer led to the lower water content.

Given the complexity of the environmental conditions, the spectroscopic analysis was still able to demonstrate the potential to predict biochemical traits. Our model accuracy of four traits in sagebrush was comparable to or higher than previous studies of nitrogen content [33]. At canopy level, only validation models of LMA and carbon content showed R -square values above 0.5 and comparable rRMSE values to calibration models. In comparison, canopy-level PLSR models of bitterbrush showed much lower prediction ability than sagebrush. Bitterbrush leaves are about 1cm long (Jepson eFlora, <http://ucjeps.berkeley.edu/eflora/>, last accessed in August 2018), but our samples showed significantly smaller leaf sizes and fragmented shape. The complex canopy structure and especially small leaves in bitterbrush makes it more difficult to spectrally estimate traits. Various methods have been used to minimize noise and resolve overlapping absorption features such as difference and logarithm transformation in reflectance [47,48]. We tested the difference and logarithm transformation and found no significant improvement for prediction (results not reported).

Our PLSR models identified high VIP values in spectral regions significantly correlated with biochemical trait variation. High VIP values in LMA models were generally located in near-infrared and short-wave infrared [13,49–51], which was associated to leaf structure and dry matter such as cellulose and lignin. Significant spectral regions in short-wave infrared were also shown in the models of carbon which was the major component in dry matter. VIP values of water models showed some

high values near 1450 and 2300 nm as identified in previous studies [52], and smaller values in spectral regions associated with dry matter. Nitrogen is a relatively small component of leaf dry matter content, with an average 1.5% in bitterbrush and 2.3% in sagebrush from our leaf samples. Kokaly [53] identified two absorption features at 2055 and 2172 nm on the shoulders of 2100 nm corresponding to absorption features of proteins. Our nitrogen models showed high VIP values in this spectral region. VIP values of four vegetation traits covered common dry matter-related wavelengths in short-wave infrared, which demonstrated that the main spectral signatures of water-stressed shrubs in this ecoregion were attributed to dry matter.

Plot-level LMA models in sagebrush showed higher *R*-square values and lower rRMSE values than canopy-level models. The nitrogen content model showed higher *R*-square value but rRMSE value increased as well. Results of water and carbon content were poorer than canopy-level models. Compared to study sites in a wetter section of the Great Basin [33], our sagebrush had a much lower nitrogen content, and shrub vegetation cover in our plots was also much lower. Many of our surveyed shrub canopies had canopy diameters that were smaller than the AVIRIS-NG data pixel size of 2.6 m. This study showed significant effects of canopy structure for remote sensing of traits. Knyazikhin et al. [54] argued the canopy structure's important role in canopy radiative transfer and spectral determination of nitrogen content in closed canopy environments. Several papers have investigated the practical limits on sparse vegetation cover discrimination in dryland environments [25], and several methods have been proposed to estimate vegetation structure and cover such as spectral unmixing and data fusion of passive and active remote sensing data [55–60]. We suggest future research should examine whether the combining airborne imaging spectrometer with a high-resolution multispectral camera or lidar sensor can better predict shrub biochemical traits over large landscapes.

5. Conclusions

The characterization of plant biochemical traits is important for understanding dryland ecosystems and their response to environmental change. To summarize our findings, this study demonstrated the performance of airborne imaging spectrometer AVIRIS-NG to estimate biochemical traits of sagebrush and bitterbrush in the Great Basin ecoregion, including leaf mass per area, water content, nitrogen content and carbon content. Sparse vegetation cover, complex canopy structure and small foliage size made the spectral estimation more challenging. The spectral regions identified by VIP values in PLSR models displayed significant distinctions in specific wavelengths corresponding to known biochemical absorption features, including those related to foliar lignin, cellulose, nitrogen, and water. A regional remote sensing estimation of vegetation canopy structure will facilitate a more robust prediction of vegetation traits. A future step will be to combine similar data sets from other shrub species to refine and standardize both data and methods as a basis to operationally estimating foliar traits in dryland ecosystems with the NEON airborne observation platform, NASA's proposed space-borne Hyperspectral Infrared Imager (HypIRI), and German EnMAP mission.

Author Contributions: Y.Q., S.L.U. and N.F.G. conceived and designed the experiments; Y.Q. had the lead in the field research and experiments; Y.Q. analyzed the data and drafted the manuscript, and all authors gave comments and revisions.

Funding: NASA Terrestrial Ecology grant NNX14AD81G.

Acknowledgments: Funding for this research was provided by NASA Terrestrial Ecology grant NNX14AD81G to Nancy F. Glenn and Susan L. Ustin. Thank you to Mui Clay, Mike Whiting, Jasmine Shen, Paul Brower, Rodger Stephens, Spencer Mathews, Chris Preston, Karine Adeline and Kristen Shapiro for field and laboratory assistance.

Conflicts of Interest: The authors declare no conflict of interest. The founding sponsors had no role in the design of the study; in the collection, analyses, or interpretation of data; in the writing of the manuscript, and in the decision to publish the results.

References

1. Melillo, J.M.; Aber, J.D.; Muratore, J.F. Nitrogen and Lignin Control of Hardwood Leaf Litter Decomposition Dynamics. *Ecology* **1982**, *63*, 621–626. [[CrossRef](#)]
2. Shipley, B.; Vile, D.; Garnier, E.; Wright, I.J.; Poorter, H. Functional linkages between leaf traits and net photosynthetic rate: reconciling empirical and mechanistic models. *Funct. Ecol.* **2005**, *19*, 602–615. [[CrossRef](#)]
3. Santiago, L.S.; Wright, S.J. Leaf functional traits of tropical forest plants in relation to growth form. *Funct. Ecol.* **2007**, *21*, 19–27. [[CrossRef](#)]
4. Cornwell, W.K.; Cornelissen, J.H.C.; Amatangelo, K.; Dorrepaal, E.; Eviner, V.T.; Godoy, O.; Hobbie, S.E.; Hoorens, B.; Kurokawa, H.; Pérez-Harguindeguy, N.; et al. Plant species traits are the predominant control on litter decomposition rates within biomes worldwide. *Ecol. Lett.* **2008**, *11*, 1065–1071. [[CrossRef](#)] [[PubMed](#)]
5. Wright, I.J.; Reich, P.B.; Westoby, M.; Ackerly, D.D.; Baruch, Z.; Bongers, F.; Cavender-Bares, J.; Chapin, T.; Cornelissen, J.H.C.; Diemer, M.; et al. The worldwide leaf economics spectrum. *Nature* **2004**, *428*, 821–827. [[CrossRef](#)] [[PubMed](#)]
6. Poorter, L. Leaf traits show different relationships with shade tolerance in moist versus dry tropical forests. *New Phytol.* **2009**, *181*, 890–900. [[CrossRef](#)] [[PubMed](#)]
7. Niinemets, Ü. Photosynthesis and resource distribution through plant canopies. *Plant Cell Environ.* **2007**, *30*, 1052–1071. [[CrossRef](#)] [[PubMed](#)]
8. Goetz, S.J.; Prince, S.D. Remote sensing of net primary production in boreal forest stands. *Agric. For. Meteorol.* **1996**, *78*, 149–179. [[CrossRef](#)]
9. Fourty, T.; Baret, F. Vegetation water and dry matter contents estimated from top-of-the-atmosphere reflectance data: A simulation study. *Remote Sens. Environ.* **1997**, *61*, 34–45. [[CrossRef](#)]
10. Kramer, P.; Boyer, J. *Water Relations of Plants and Soils*; Academic Press: Cambridge, MA, USA, 1995; p. 495.
11. Field, C.; Mooney, H. The photosynthesis-nitrogen relationship in wild plants. In *on the Economy of Plant Form and Function*; Givnish, T., Ed.; Cambridge University Press: Cambridge, UK, 1986; pp. 25–55.
12. Reich, P.B.; Walters, M.B.; Ellsworth, D.S. Leaf Life-Span in Relation to Leaf, Plant, and Stand Characteristics among Diverse Ecosystems. *Ecol. Monogr.* **1992**, *62*, 365–392. [[CrossRef](#)]
13. Kokaly, R.F.; Asner, G.P.; Ollinger, S.V.; Martin, M.E.; Wessman, C.A. Characterizing canopy biochemistry from imaging spectroscopy and its application to ecosystem studies. *Remote Sens. Environ.* **2009**, *113*, S78–S91. [[CrossRef](#)]
14. Ustin, S.L.; Roberts, D.A.; Gamon, J.A.; Asner, G.P.; Green, R.O. Using imaging spectroscopy to study ecosystem processes and properties. *BioScience* **2004**, *54*, 523–534. [[CrossRef](#)]
15. Asner, G.; Martin, R. Spectral and chemical analysis of tropical forests: Scaling from leaf to canopy levels. *Remote Sens. Environ.* **2008**, *112*, 3958–3970. [[CrossRef](#)]
16. Asner, G.P.; Martin, R.E.; Knapp, D.E.; Tupayachi, R.; Anderson, C.B.; Sinca, F.; Vaughn, N.R.; Llactayo, W. Airborne laser-guided imaging spectroscopy to map forest trait diversity and guide conservation. *Science* **2017**, *355*, 385. [[CrossRef](#)] [[PubMed](#)]
17. Singh, A.; Serbin, S.P.; McNeil, B.E.; Kingdon, C.C.; Townsend, P.A. Imaging spectroscopy algorithms for mapping canopy foliar chemical and morphological traits and their uncertainties. *Ecol. Appl.* **2015**, *25*, 2180–2197. [[CrossRef](#)] [[PubMed](#)]
18. Serbin, S.P.; Singh, A.; McNeil, B.E.; Kingdon, C.C.; Townsend, P.A. Spectroscopic determination of leaf morphological and biochemical traits for northern temperate and boreal tree species. *Ecol. Appl.* **2014**, *24*, 1651–1669. [[CrossRef](#)]
19. Serrano, L.; Peñuelas, J.; Ustin, S.L. Remote sensing of nitrogen and lignin in Mediterranean vegetation from AVIRIS data: Decomposing biochemical from structural signals. *Remote Sens. Environ.* **2002**, *81*, 355–364. [[CrossRef](#)]
20. Roberts, D.A.; Dennison, P.E.; Peterson, S.; Sweeney, S.; Rechel, J. Evaluation of Airborne Visible/Infrared Imaging Spectrometer (AVIRIS) and Moderate Resolution Imaging Spectrometer (MODIS) measures of live fuel moisture and fuel condition in a shrubland ecosystem in southern California. *J. Geophys. Res.* **2006**, *111*. [[CrossRef](#)]
21. Roberts, D.A.; Ustin, S.L.; Ogunjemiyo, S.; Greenberg, J.; Bobrowski, S.Z.; Chen, J.; Hinckley, T.M. Spectral and structural measures of northwest forest vegetation at leaf to landscape scales. *Ecosystems* **2004**, *7*, 545–562. [[CrossRef](#)]

22. Yang, X.; Tang, J.; Mustard, J.F.; Wu, J.; Zhao, K.; Serbin, S.; Lee, J.-E. Seasonal variability of multiple leaf traits captured by leaf spectroscopy at two temperate deciduous forests. *Remote Sens. Environ.* **2016**, *179*, 1–12. [[CrossRef](#)]
23. Asner, G.P.; Wessman, C.A.; Bateson, C.A.; Privette, J.L. Impact of tissue, canopy, and landscape factors on the Hyperspectral reflectance variability of arid ecosystems. *Remote Sens. Environ.* **2000**, *74*, 69–84. [[CrossRef](#)]
24. Smith, M.O.; Ustin, S.L.; Adams, J.B.; Gillespie, A.R. Vegetation in deserts: I. A regional measure of abundance from multispectral images. *Remote Sens. Environ.* **1990**, *31*, 1–26. [[CrossRef](#)]
25. Okin, G.S.; Roberts, D.A.; Murray, B.; Okin, W.J. Practical limits on hyperspectral vegetation discrimination in arid and semiarid environments. *Remote Sens. Environ.* **2001**, *77*, 212–225. [[CrossRef](#)]
26. Ustin, S.L.; Smith, M.O.; Adams, J.B. A strategy for Developing Ecological Models Using Spectral Mixture Analysis. In *Scaling Physiological Processes: Leaf to Globe*; Ehleringer, J., Field, C., Eds.; Academic Press: Cambridge, MA, USA, 1993; pp. 339–357.
27. Grossman, Y.L.; Ustin, S.L.; Jacquemoud, S.; Sanderson, E.W.; Schmuck, G.; Verdebout, J. Critique of stepwise multiple linear regression for the extraction of leaf biochemistry information from leaf reflectance data. *Remote Sens. Environ.* **1996**, *56*, 182–193. [[CrossRef](#)]
28. Næsset, E.; Bollandsås, O.M.; Gobakken, T. Comparing regression methods in estimation of biophysical properties of forest stands from two different inventories using laser scanner data. *Remote Sens. Environ.* **2005**, *94*, 541–553. [[CrossRef](#)]
29. Asner, G.P.; Martin, R.E.; Anderson, C.B.; Knapp, D.E. Quantifying forest canopy traits: Imaging spectroscopy versus field survey. *Remote Sens. Environ.* **2015**, *158*, 15–27. [[CrossRef](#)]
30. Ustin, S.L.; Roberts, D.A.; Pinzón, J.; Jacquemoud, S.; Gardner, M.; Scheer, G.; Castañeda, C.M.; Palacios-Orueta, A. Estimating canopy water content of chaparral shrubs using optical methods. *Remote Sens. Environ.* **1998**, *65*, 280–291. [[CrossRef](#)]
31. Serrano, L.; Ustin, S.L.; Roberts, D.A.; Gamon, J.A.; Peñuelas, J. Deriving water content of chaparral vegetation from AVIRIS data. *Remote Sens. Environ.* **2000**, *74*, 570–581. [[CrossRef](#)]
32. Mirik, M.; Norland, J.E.; Crabtree, R.L.; Biondini, M.E. Hyperspectral One-Meter-Resolution Remote Sensing in Yellowstone National Park, Wyoming: I. Forage Nutritional Values. *Rangel. Ecol. Manag.* **2005**, *58*, 452–458. [[CrossRef](#)]
33. Mitchell, J.J.; Glenn, N.F.; Sankey, T.T.; Derryberry, D.R.; Germino, M.J. Remote sensing of sagebrush canopy nitrogen. *Remote Sens. Environ.* **2012**, *124*, 217–223. [[CrossRef](#)]
34. Reynolds, J.F.; Smith, D.M.S.; Lambin, E.F.; Turner, B.L.; Mortimore, M.; Batterbury, S.P.J.; Downing, T.E.; Dowlatabadi, H.; Fernandez, R.J.; Herrick, J.E.; et al. Global Desertification: Building a Science for Dryland Development. *Science* **2007**, *316*, 847–851. [[CrossRef](#)] [[PubMed](#)]
35. Balch, J.K.; Bradley, B.A.; D’Antonio, C.M.; Gómez-Dans, J. Introduced annual grass increases regional fire activity across the arid western USA (1980–2009). *Glob. Chang. Boil.* **2013**, *19*, 173–183. [[CrossRef](#)] [[PubMed](#)]
36. Cook, E.R.; Woodhouse, C.A.; Eakin, C.M.; Meko, D.M.; Stahle, D.W. Long-Term Aridity Changes in the Western United States. *Science* **2004**, *306*, 1015–1018. [[CrossRef](#)] [[PubMed](#)]
37. Asner, G.P.; Brodrick, P.G.; Anderson, C.B.; Vaughn, N.; Knapp, D.E.; Martin, R.E. Progressive forest canopy water loss during the 2012–2015 California drought. *Proc. Natl. Acad. Sci. USA* **2016**, *113*, E249–E255. [[CrossRef](#)] [[PubMed](#)]
38. Xue, T.; Tang, G.; Sun, L.; Wu, Y.; Liu, Y.; Dou, Y. Long-term trends in precipitation and precipitation extremes and underlying mechanisms in the U.S. Great Basin during 1951–2013. *J. Geophys. Res. Atmos.* **2017**, *122*, 6152–6169. [[CrossRef](#)]
39. Kampe, T.U.; Asner, G.P.; Green, R.O.; Eastwood, M.; Johnson, B.R.; Kuester, M. Advances in airborne remote sensing of ecosystem processes and properties—Toward high-quality measurement on a global scale. *Proc. SPIE* **2010**, *7809*, 7809–7813.
40. Gao, B.-C.; Heidebrecht, K.B.; Goetz, A.F.H. Derivation of scaled surface reflectances from AVIRIS data. *Remote Sens. Environ.* **1993**, *44*, 165–178. [[CrossRef](#)]
41. Martens, H.; Naes, T. Multivariate calibration by data compression. In *Near-Infrared Technology in the Agriculture and Food Industries*, 2nd ed.; Norris, W., Norris, K., Eds.; American Association of Cereal Chemists: St. Paul, MN, USA, 2001; pp. 59–100.
42. Qi, Y.; Dennison, P.E.; Jolly, W.M.; Kropp, R.C.; Brewer, S.C. Spectroscopic analysis of seasonal changes in live fuel moisture content and leaf dry mass. *Remote Sens. Environ.* **2014**, *150*, 198–206. [[CrossRef](#)]

43. Kennard, R.W.; Stone, L.A. Computer Aided Design of Experiments. *Technometrics* **1969**, *11*, 137–148. [[CrossRef](#)]
44. Wold, S.; Sjöström, M.; Eriksson, L. PLS-regression: a basic tool of chemometrics. *Chemom. Intell. Lab. Syst.* **2001**, *58*, 109–130. [[CrossRef](#)]
45. Mehmood, T.; Liland, K.H.; Snipen, L.; Sæbø, S. A review of variable selection methods in Partial Least Squares Regression. *Chemom. Intell. Lab. Syst.* **2012**, *118*, 62–69. [[CrossRef](#)]
46. Dina, S.J.; Klikoff, L.G. Effect of Plant Moisture Stress on Carbohydrate and Nitrogen Content of Big Sagebrush. *J. Range Manag.* **1973**, *26*, 207–209. [[CrossRef](#)]
47. Bolster, K.L.; Martin, M.E.; Aber, J.D. Determination of carbon fraction and nitrogen concentration in tree foliage by near infrared reflectances: a comparison of statistical methods. *Can. J. For. Res.* **1996**, *26*, 590–600. [[CrossRef](#)]
48. Ourcival, J.M.; Joffre, R.; Rambal, S. Exploring the relationships between reflectance and anatomical and biochemical properties in *Quercus ilex* leaves. *New Phytol.* **1999**, *143*, 351–364. [[CrossRef](#)]
49. Asner, G.P.; Martin, R.E.; Tupayachi, R.; Emerson, R.; Martinez, P.; Sinca, F.; Powell, G.V.N.; Wright, S.J.; Lugo, A.E. Taxonomy and remote sensing of leaf mass per area (LMA) in humid tropical forests. *Ecol. Appl.* **2011**, *21*, 85–98. [[CrossRef](#)] [[PubMed](#)]
50. Serbin, S.P.; Dillaway, D.N.; Kruger, E.L.; Townsend, P.A. Leaf optical properties reflect variation in photosynthetic metabolism and its sensitivity to temperature. *J. Exp. Bot.* **2012**, *63*, 489–502. [[CrossRef](#)] [[PubMed](#)]
51. Cheng, T.; Rivard, B.; Sánchez-Azofeifa, A.G.; Féret, J.-B.; Jacquemoud, S.; Ustin, S.L. Deriving leaf mass per area (LMA) from foliar reflectance across a variety of plant species using continuous wavelet analysis. *ISPRS J. Photogramm. Remote Sens.* **2014**, *87*, 28–38. [[CrossRef](#)]
52. Kokaly, R.F.; Clark, R.N. Spectroscopic determination of leaf biochemistry using band-depth analysis of absorption features and stepwise multiple linear regression. *Remote Sens. Environ.* **1999**, *67*, 267–287. [[CrossRef](#)]
53. Kokaly, R.F. Investigating a physical basis for spectroscopic estimates of leaf nitrogen concentration. *Remote Sens. Environ.* **2001**, *75*, 153–161. [[CrossRef](#)]
54. Knyazikhin, Y.; Schull, M.A.; Stenberg, P.; Mörtus, M.; Rautiainen, M.; Yang, Y.; Marshak, A.; Latorre Carmona, P.; Kaufmann, R.K.; Lewis, P.; et al. Hyperspectral remote sensing of foliar nitrogen content. *Proc. Natl. Acad. Sci. USA* **2013**, *110*, E185–E192. [[CrossRef](#)] [[PubMed](#)]
55. Asner, G.P.; Heidebrecht, K.B. Spectral unmixing of vegetation, soil and dry carbon cover in arid regions: Comparing multispectral and hyperspectral observations. *Int. J. Remote Sens.* **2002**, *23*, 3939–3958. [[CrossRef](#)]
56. Huang, S.; Potter, C.; Crabtree, R.L.; Hager, S.; Gross, P. Fusing optical and radar data to estimate sagebrush, herbaceous, and bare ground cover in Yellowstone. *Remote Sens. Environ.* **2010**, *114*, 251–264. [[CrossRef](#)]
57. McGwire, K.; Minor, T.; Fenstermaker, L. Hyperspectral Mixture Modeling for Quantifying Sparse Vegetation Cover in Arid Environments. *Remote Sens. Environ.* **2000**, *72*, 360–374. [[CrossRef](#)]
58. Guerschman, J.P.; Hill, M.J.; Renzullo, L.J.; Barrett, D.J.; Marks, A.S.; Botha, E.J. Estimating fractional cover of photosynthetic vegetation, non-photosynthetic vegetation and bare soil in the Australian tropical savanna region upscaling the EO-1 Hyperion and MODIS sensors. *Remote Sens. Environ.* **2009**, *113*, 928–945. [[CrossRef](#)]
59. Mundt, J.T.; Streutker, D.R.; Glenn, N.F. Mapping Sagebrush Distribution Using Fusion of Hyperspectral and Lidar Classifications. *Photogramm. Eng. Remote Sens.* **2006**, *72*, 47–54. [[CrossRef](#)]
60. Mitchell, J.J.; Shrestha, R.; Spaete, L.P.; Glenn, N.F. Combining airborne hyperspectral and LiDAR data across local sites for upscaling shrubland structural information: Lessons for HypSIRI. *Remote Sens. Environ.* **2015**, *167*, 98–110. [[CrossRef](#)]

